







Article

Designing an Efficient Surfactant–Polymer–Oil–Electrolyte System: A Multi-Objective Optimization Study

Mohammed Nedjhioui ¹, Nouredine Nasrallah ², Mohammed Kebir ³, Hichem Tahraoui ^{4,5,*}, Rachida Bouallouche ², Aymen Amin Assadi ^{6,7}, Abdeltif Amrane ^{6,*}, Bassem Jaouadi ⁸, Jie Zhang ⁹ and Lotfi Mouni ¹⁰

- ¹ Materials and Environment Laboratory (LME), Faculty of Technology, Yahia Feres University, Medea 26000, Algeria
- ² Reaction Engineering Laboratory, Faculty of Mechanical and Process Engineering, University of Science and Technology Houari Boumediene, BP32 El Alia, Bab Ezzouar, Algiers 16111, Algeria
- ³ Research Unit on Analysis and Technological Development in Environment (UR-ADTE/CRAPC), BP 384 Bou-Ismaïl, Tipaza 42000, Algeria
- ⁴ Laboratoire de Génie des Procédés Chimiques, Department of Process Engineering, University of Ferhat Abbas, Setif 19000, Algeria
- ⁵ Laboratoire de Biomatériaux et Phénomènes de Transports (LBMPT), Université Yahia Fares de Médéa Pôle Urbain, Medea 26000, Algeria
- ⁶ National Center for Scientific Research (CNRS), National School of Chemistry of Rennes, University of Rennes, ISCR—UMR6226, F-35000 Rennes, France
- ⁷ Department of Chemistry, Al Imam Mohammad Ibn Saud Islamic University (IMISIU), P.O. Box 5701, Riyadh 11432, Saudi Arabia
- ⁸ Laboratoire de Biotechnologie Microbienne, Enzymatique et de Biomolécules (LBMEB), Centre de Biotechnologie de Sfax (CBS), Université de Sfax, Sfax 3018, Tunisia
- ⁹ School of Chemical Engineering and Advanced Materials, Newcastle University, Newcastle upon Tyne NE1 7RU, UK
- ¹⁰ Laboratory of Management and Valorization of Natural Resources and Quality Assurance, SNVST Faculty, University of Bouira, Bouira 10000, Algeria
- * Correspondence: hichemm.tahraoui@gamil.com (H.T.); abdeltif.amrane@univ-rennes1.fr (A.A.)



Citation: Nedjhioui, M.; Nasrallah, N.; Kebir, M.; Tahraoui, H.; Bouallouche, R.; Assadi, A.A.; Amrane, A.; Jaouadi, B.; Zhang, J.; Mouni, L. Designing an Efficient Surfactant–Polymer–Oil–Electrolyte System: A Multi-Objective Optimization Study. *Processes* **2023**, *11*, 1314. <https://doi.org/10.3390/pr11051314>

Academic Editors: Giannis Penoglou and Alexandros Kiparissides

Received: 17 March 2023

Revised: 17 April 2023

Accepted: 20 April 2023

Published: 24 April 2023



Copyright: © 2023 by the authors. Licensee MDPI, Basel, Switzerland. This article is an open access article distributed under the terms and conditions of the Creative Commons Attribution (CC BY) license (<https://creativecommons.org/licenses/by/4.0/>).

Abstract: This research aimed to study the effects of individual components on the physicochemical properties of systems composed of surfactants, polymers, oils, and electrolytes in order to maximize the recovery efficiency of kerosene while minimizing the impact on the environment and human health. Four independent factors, namely anionic surfactant sodium dodecylbenzene sulfonate (X_1) (SDBS), oil (X_2) (kerosene), water-soluble polymer poly(ethylene glycol) (X_3) (PEG), and sodium chloride (X_4) (NaCl), were studied using the full factorial design (FFD) model. Four output variables, namely conductivity (Y_1), turbidity (Y_2), viscosity (Y_3), and interfacial tension (IFT) (Y_4), were taken as the response variables. All four FFD models have high coefficients of determination and low errors. The developed models were used in a multi-objective optimization (MOO) framework to determine the optimal conditions. The obtained optimal conditions are $X_1 = 0.01$, $X_2 = 50$, $X_3 = 5$, and $X_4 = 0.1$, with an error of 0.9414 between the predicted and experimental objective function values. This result shows the efficiency of the model developed and the system used for the recovery of kerosene, while also having a positive effect on the protection of the environment.

Keywords: polymer; full factorial design; conductivity; interfacial tension; turbidity; viscosity

1. Introduction

Mixtures containing surfactants, polymers, and oil, as well as electrolytes, are widely used in various industries, including wastewater treatment, cosmetics, food, paints, detergents, pesticides, and even in polymer synthesis processes. The practical application of these surfactant/polymer/oil combinations has become necessary in many situations. For instance, the petroleum industry uses surfactant and polymer combinations to enhance

oil recovery. The interaction between water-soluble polymers, surfactants, and oil has a significant impact on the behavior of the polymer/surfactant/oil system in terms of its mobility and viscosity. The primary purpose of using polymers is to reduce the mobility of the aqueous phase, which, in turn, increases its viscosity [1,2]. The rheological and physicochemical properties of solutions containing polymers and surfactants can be impacted by the interactions of molecules within them [3]. The characteristics of these interactions are influenced by various factors, such as the electrical charges and hydrophobicity of both the polymer and surfactant, the conformation and flexibility of the polymer, and the presence of additives such as salts. Typically, the hydrophobic nature of the polymer and surfactant is the primary cause of these interactions [4]. The study of these interactions has been ongoing for many years and is well-documented [5]. Although not yet fully comprehended, these interactions exhibit substantial variations in the physicochemical and rheological properties of the systems. The majority of research in this area centers on the complexes formed between anionic surfactants and polymers [6–8]. In the mining industry, these combinations are used to improve flotation and mineral separation processes. Surfactants are used as collectors to float valuable minerals, while polymers modify the viscosity and stability of emulsions, and oils act as lubricants to reduce friction and facilitate separation processes [9,10]. These combinations are also used in other industries, such as the production of cosmetics, food, paints, detergents, and pesticides. In wastewater treatment, these combinations are used to aid in the separation of solids and liquids and to remove contaminants from water. Overall, the unique properties and effectiveness of these surfactant/polymer/oil combinations make them an essential component of many industrial processes [9,10].

There are two approaches to examining the combined effects of a surfactant and a micellar system containing a surfactant, oil, polymer, and electrolyte. The first approach considers the polymer as the substance affected by the surfactant, while the second approach considers the surfactant as the substance influenced by the polymer. In the first approach, the surfactant adsorbs onto the polymer sites, disrupting the formation of surfactant micelles. In contrast, the second approach involves the association of surfactant molecules with macromolecules, thus facilitating micellization [11,12]. Studying the changes in physicochemical and rheological properties in these systems based on the concentrations and chemical nature of their components can reveal relationships between these factors and system responses such as conductivity, turbidity, and critical micelle concentration. To minimize testing while maximizing reliability, experimental plans are carried out to obtain predictive models of the studied responses and optimal conditions. For the objective of determining the effects of three constituents, the most suitable experimental planning strategy involves response surface methodology (RSM) using a second-order polynomial model that takes into account all first- and second-order interactions between the factors. Experimental planning encompasses statistical techniques that analyze the behavior of experimental systems, providing insights for improving their performance. In particular, in the industrial field, experimental designs are continually developed and can be used to optimize manufacturing and control processes and formulate products [13]. Experiment plans are used to streamline the testing process, allowing for maximum information to be obtained with minimal testing. This approach also enhances precision in modeling results. Experimental design methodology is based on strict mathematical principles, necessitating a meticulous approach from the experimenter [13–16].

Previously, researchers utilized the one-factor-at-a-time experimental approach, which was not only more time-consuming and costly, but also neglected the impact of interactions between factors. Although the conventional orthogonal method could consider several factors simultaneously, it is unable to determine a functional relationship between the factors and response values. Experimental design is a statistical method that utilizes quantitative data from suitable experiments to establish multiple regression equations between the factors and experimental outcomes. The primary advantage of this approach over other statistical experimental design methods is the decreased number of experiment

trials required to assess multiple parameters and their interactions [17]. Full factorial designs are systematic and uncomplicated designs that allow for the evaluation of the primary effects and interactions [18]. When dealing with a large number of variables or many levels of a factor, the required number of test points in the full factorial design grows exponentially. To address this, researchers typically start with a basic layout, such as a full factorial or partial factorial design. A popular example is the 2^k factorial design, where each factor has only two values. This approach helps to analyze both the main effects and the interactions of independent variables, including both categorical and continuous components [19]. The factors that impact the process are referred to as independent variables, while the outcomes are referred to as dependent variables [20].

The use of certain combinations of an anionic surfactant, polymer, oil, and electrolyte can have adverse environmental and human health consequences due to the presence of toxic compounds or their accumulation in the environment. Research is currently underway to develop more environmentally friendly and sustainable suits for these industrial applications. This study aimed to evaluate the potential of an anionic surfactant, polymer, oil, and electrolyte system on physicochemical properties such as conductivity, turbidity, viscosity, and interfacial tension by optimizing the processing conditions through full factorial design. In order to achieve both maximum kerosene recovery efficiency and minimal environmental and health impact, a novel multi-objective optimization approach utilizing the particle swarm technique (PSO) was employed to determine the optimal process conditions for all outputs simultaneously. This study also represents the first attempt to optimize the effectiveness of a system involving anionic surfactant, polymer, oil, and sodium chloride components on physicochemical properties using FFD. Furthermore, the application of a multi-objective optimization approach to maximize kerosene recovery efficiency while minimizing its environmental and health impact and identifying the optimal processing conditions for all outputs has not been previously explored in this context.

2. Materials and Methods

2.1. Chemicals

This research project employed several chemical substances, including sodium dodecylbenzene sulphonate (SDBS), an anionic surfactant with the formula (C₁₂H₂₅C₆H₄SO₃Na); kerosene, a combination of hydrocarbons containing alkanes (C_nH_{2n+2}), with a chemical composition ranging from C₁₀H₂₂ to C₁₄H₃₀; polyethylene glycol (PEG), with the formula C_{2n}H_{4n+2}O_{n+1}; and sodium chloride (NaCl). SDBS was procured from Rhodia, in France, while kerosene (with a density and kinematic viscosity of 775 kg/m³ and 6.2 × 10⁻³ Pa.s, respectively) and crude oil (with a density 806 kg/m³ and viscosity 22 × 10⁻³ Pa.s.) were acquired from an Algerian oil field. The polymer used, PEG 1500, was supplied by Sigma and has an average molecular weight of 1500. Finally, sodium chloride (NaCl) with a reagent grade purity of 99% was obtained from Panreac, in Spain [19–21].

2.2. Full Factorial Design

The full factorial design (FFD) is a method of generating experimental points by considering all possible combinations of factor levels in each full trial or experimental replication. In an FFD, the experimental points are located at the corners of a hexagonal lattice within the *n*-dimensional construction region, which is defined by the minimum and maximum values for each component. These specific experimental points are commonly referred to as factorial points [19–24]. An integer factorial run for four two-level factors generates 2⁴ experimental points and 3 center points, resulting in a total of 19 design experiments. The FFD allows a full evaluation of all possible combinations of input variables or factors and their levels, thus providing a comprehensive understanding of the relationship between the input variables and the output responses. This means that the entire experimental space can be explored, thus allowing the identification of significant factors and their interactions, as well as the determination of the optimal levels of input variables for obtaining the desired output response [13].

In this context, FFD was employed with four independent parameters—the mass concentration of SDBS, the mass concentration of kerosene, the mass concentration of PEG 1500, and the mass concentration of NaCl. Additionally, four output parameters were considered, namely conductivity, turbidity, viscosity, and interfacial tension. The statistical analysis was performed using the JMP program (version 13 pro), with the range of independent variables selected based on preliminary studies. The range of independent parameters for this study are as follows:

- X_1 : mass concentration of SDBS, which varies between [0.01 w% and 0.08 w%].
- X_2 : mass concentration of kerosene, which varies between [20 w% and 50 w%].
- X_3 : mass concentration of PEG 1500, which varies between [5 w% and 20 w%].
- X_4 : mass concentration of NaCl, ranges from [0.1 w% to 2 w%].
- Y_1 : conductivity (mS/cm); Y_2 : turbidity (NTU); Y_3 : viscosity (mPa.s); and Y_4 : interfacial tension (mN/m).

The electrical conductivity of the solutions was measured using an EC 214 type of conductimeter (Hanna instruments) with a constant cell of 0.475 cm^{-1} . The measurement scale consists of two ranges: the first range can measure values of electrical conductivity between 199 and 1999 $\mu\text{S/cm}$, while the second range allows measurements between 19.99 and 199.9 mS/cm. Turbidimetric measurements were conducted using the “WTW turbo 550 IR” turbidimeter, with a reference no. of 600110, which has a measurement range of 0.001 to 1000 Nephelometric Turbidimetric Unit NUT. The Haak RVT5 viscometer was utilized to measure the viscosity of Newtonian liquids. It comes with six mobiles of varying shapes and geometry, and each mobile has a specific range of viscosity and shear speed, with the latter varying between 0.3 and 200 R.P.M (min^{-1}). Additionally, the interfacial tensions and critical aggregation concentrations of the mixtures were measured using a Du Noüy tensiometer model 70,545 (CSC Scientific Co., VA, USA) through a surface tension method. Polymer dispersions were prepared by dissolving the polymer in water, with mild stirring, at room temperature, followed by the addition of different amounts of surfactant and oil to the polymer solutions. The surfactant was dissolved in a helix mixer (Heidolph RZR 2020, Germany) at concentrations higher or lower than the critical micelle concentration (cmc) of the surfactant, depending on the case. The polymer concentrations were varied to induce changes in the solution’s viscosimetric and turbidimetric properties [12,25,26].

2.3. Statistical Evaluation Criteria

The quality of the developed models was examined using statistical analysis and ANOVA at a 95% confidence level. Various model quality measures, such as the p -value, F-value, degree of freedom (DF), coefficient of determination (R^2), adjusted determination of coefficient (R_{adj}^2), and Root Mean Square Error (RMSE), were used to evaluate the statistical adequacy of the models [15,25,27–35]. The F-value describes the variation in the responses, which can be evaluated using a regression equation, whereas the p -value indicates the statistical adequacy of the developed model. A model is considered significant if the p -value is less than 5%, and the p -value for the inadequacy test should be greater than 5% [28].

3. Results and Discussion

3.1. Full Factorial Design Modeling

The quality of the developed FFD models was analyzed using the software “JMP 13 pro”. This method established a mathematical equation (Equation (1)) linking four input variables, i.e., SDBS concentration, kerosene concentration, PEG, and sodium chloride concentration, to four output variables: conductivity (mS/cm), turbidity (NTU), viscosity (mPa.s), and interfacial tension (mN/m). Table 1 presents the outcomes of 19 experiments conducted in the laboratory. It is important to note that the final concentrations of the output variables (conductivity, turbidity, viscosity, and interfacial tension) were used in the analysis.

Table 1. Set of experimental conditions of independent variables and responses.

Experience N°	SDBS (%w)	Kerosene (%w)	PEG (%w)	NaCl (%w)	Conductivity (mS/cm)	Turbidity (NTU)	Viscosity (mPa.s)	Interfacial Tension (mN/m)
1	0.01	20	5	0.1	2.8	101	170	37.6
2	0.08	20	5	0.1	3.3	111	200	36.8
3	0.01	50	5	0.1	3.4	127	220	37.2
4	0.08	50	5	0.1	3.6	134	240	35
5	0.01	20	20	0.1	3.8	132	255	34.9
6	0.08	20	20	0.1	4.2	134	275	34.5
7	0.01	50	20	0.1	3.9	180	294	35.5
8	0.08	50	20	0.1	4.3	184	324	35.6
9	0.01	20	5	2	3.2	174	241	35.1
10	0.08	20	5	2	3.3	182	257	34.2
11	0.01	50	5	2	3.7	181	284	34.8
12	0.08	50	5	2	4.1	186	309	33.6
13	0.01	20	20	2	3.9	191	301	31.6
14	0.08	20	20	2	4.1	198	320	31.5
15	0.01	50	20	2	4.1	224	334	32.8
16	0.08	50	20	2	4.3	225	360	32.4
17	0.045	35	12.5	1.05	3.7	167	275	34.7
18	0.045	35	12.5	1.05	3.8	165	270	34
19	0.045	35	12.5	1.05	3.7	166	275	34.7

The statistical information required for the development and comprehension of the FFD model is presented in Table 2. Equation (1) represents the relationship between the four input variables, including their interactions, and the four output variables.

$$Y = \beta_0 + \beta_1 X_1 + \beta_2 X_2 + \beta_3 X_3 + \beta_4 X_4 + \beta_5 X_1 X_2 + \beta_6 X_1 X_3 + \beta_7 X_2 X_3 + \beta_8 X_1 X_4 + \beta_9 X_2 X_4 + \beta_{10} X_3 \quad (1)$$

Table 2. Results of the FFD.

I	Term	β_i	Std Error	t Ratio	Prob > t	β_i	Std Error	t Ratio	Prob > t
		a. Conductivity (mS/cm)				b. Turbidity (NTU)			
0	Constant	<u>3.7473684</u>	<u>0.019427</u>	<u>192.89</u>	<u><0.0001</u>	<u>166.42105</u>	<u>0.293925</u>	<u>566.20</u>	<u><0.0001</u>
1	X ₁	<u>0.15</u>	<u>0.021171</u>	<u>7.09</u>	<u>0.0001</u>	<u>2.75</u>	<u>0.320297</u>	<u>8.59</u>	<u><0.0001</u>
2	X ₂	<u>0.175</u>	<u>0.021171</u>	<u>8.27</u>	<u><0.0001</u>	<u>13.625</u>	<u>0.320297</u>	<u>42.54</u>	<u><0.0001</u>
3	X ₃	<u>0.325</u>	<u>0.021171</u>	<u>15.35</u>	<u><0.0001</u>	<u>17</u>	<u>0.320297</u>	<u>53.08</u>	<u><0.0001</u>
4	X ₄	<u>0.0875</u>	<u>0.021171</u>	<u>4.13</u>	<u>0.0033</u>	<u>28.625</u>	<u>0.320297</u>	<u>89.37</u>	<u><0.0001</u>
5	X ₁ × X ₂	0	0.021171	0.00	1.0000	−0.625	0.320297	−1.95	0.0868
6	X ₁ × X ₃	5.551.10 ^{−17}	0.021171	0.00	1.0000	−1	0.320297	−3.12	0.0142
7	X ₂ × X ₃	−0.1	0.021171	−4.72	0.0015	6.125	0.320297	19.12	<0.0001
8	X ₁ × X ₄	−0.0375	0.021171	−1.77	0.1145	−0.125	0.320297	−0.39	0.7065
9	X ₂ × X ₄	0.0375	0.021171	1.77	0.1145	−4.75	0.320297	−14.83	<0.0001
10	X ₃ × X ₄	−0.0625	0.021171	−2.95	0.0184	−2.625	0.320297	−8.20	<0.0001

Table 2. Cont.

I	Term	β_i	Std Error	t Ratio	Prob > t	β_i	Std Error	t Ratio	Prob > t
		c. Viscosity (mPa.s)				d. Interfacial tension (mN/m)			
0	Constant	<u>273.89474</u>	<u>0.851815</u>	<u>321.54</u>	<u><0.0001</u>	<u>34.552632</u>	<u>0.078477</u>	<u>440.29</u>	<u><0.0001</u>
1	X_1	<u>11.625</u>	<u>0.928244</u>	<u>12.52</u>	<u><0.0001</u>	<u>-0.36875</u>	<u>0.085519</u>	<u>-4.31</u>	<u>0.0026</u>
2	X_2	<u>21.625</u>	<u>0.928244</u>	<u>23.30</u>	<u><0.0001</u>	0.04375	0.085519	0.51	0.6228
3	X_3	<u>33.875</u>	<u>0.928244</u>	<u>36.49</u>	<u><0.0001</u>	<u>-0.96875</u>	<u>0.085519</u>	<u>-11.33</u>	<u><0.0001</u>
4	X_4	<u>26.75</u>	<u>0.928244</u>	<u>28.82</u>	<u><0.0001</u>	<u>-1.31875</u>	<u>0.085519</u>	<u>-15.42</u>	<u><0.0001</u>
5	$X_1 \times X_2$	1	0.928244	1.08	0.3128	-0.09375	0.085519	-1.10	0.3049
6	$X_1 \times X_3$	0.25	0.928244	0.27	0.7945	<u>0.26875</u>	<u>0.085519</u>	<u>3.14</u>	<u>0.0138</u>
7	$X_2 \times X_3$	-1.5	0.928244	-1.62	0.1448	<u>0.43125</u>	<u>0.085519</u>	<u>5.04</u>	<u>0.0010</u>
8	$X_1 \times X_4$	-0.875	0.928244	-0.94	0.3735	0.04375	0.085519	0.51	0.6228
9	$X_2 \times X_4$	-0.625	0.928244	-0.67	0.5197	0.10625	0.085519	1.24	0.2493
10	$X_3 \times X_4$	<u>-5.875</u>	<u>0.928244</u>	<u>-6.33</u>	<u>0.0002</u>	<u>-0.20625</u>	<u>0.085519</u>	<u>-2.41</u>	<u>0.0424</u>

Equation (1) includes four independent variables, X_1 , X_2 , X_3 , and X_4 , which represent the SDBS concentration, kerosene concentration, PEG, and sodium chloride concentration, respectively. The response variable is Y , and the model parameters are β_0 to β_{10} . Afterward, the model parameters with a high explanatory power ($PR < 5\%$) were kept and are shown in bold and underlined in Table 2 [15]. Conversely, the other parameters with $PR > 5\%$ were removed, and the resulting models are represented by the equations in Table 3.

Table 3. FFD performances.

Final Equation in Terms of Code of Independent Variables	p	F	R^2	R^2_{adj}	RMSE
1. Conductivity (mS/cm)					
$Y1 = 3.7473 + 0.15X1 + 0.175X2 + 0.325X3 + 0.0875X4 - 0.1X2 \times X3 - 0.0625X3 \times X4$	0.3097	0.9978	0.980502	0.9561	0.0847
2. Turbidity (NTU)					
$Y2 = 166.4210 + 2.75X1 + 13.625X2 + 17X3 + 28.625X4 - X1 \times X3 + 6.125X2X3 - 4.75X \times X4 - 2.625X3 \times X4$	0.3909	1.8553	0.9991	0.9979	1.2812
3. Viscosity (mPa.s)					
$Y3 = 273.8947 + 11.625X1 + 21.625X2 + 33.875X3 + 26.75X4 - 5.875X3 \times X4$	0.3883	1.8527	0.9963	0.9917	3.7130
4. Interfacial tension (mN/m)					
$Y4 = 43.5526 - 0.3687X1 - 0.9687X3 - 1.3187X4 + 0.2687X1 \times X3 - 0.2062X3 \times X4$	0.7241	0.6219	0.9816	0.9588	0.3421

The statistical analysis indicated that certain interactions between the input parameters in the conductivity, turbidity, viscosity, and interfacial tension models were not significant since their p -value was greater than 5%, as shown in Table 2. Specifically, the interactions between X_1 and X_2 , X_1 and X_3 , X_1 and X_4 , and X_2 and X_4 in the conductivity model; between X_1 and X_2 , X_1 , and X_4 in the turbidity model; and all interactions except for the interaction between X_3 and X_4 in the viscosity model were found to be non-significant. Additionally, the interaction of X_2 in the interfacial tension model was also non-significant, and the interactions of X_1 and X_2 , X_1 and X_4 , and X_2 and X_4 were found to be non-significant. As shown in Table 3, the FFD model's performance was evaluated in terms of errors and agreement vector values.

After eliminating the low explanatory power variables, the model equations became simpler, but with a slight decrease in the values of the coefficients of determination. These coefficients show that the model has moderate positive correlations, as shown in Figure 1.

The probability value was less than 0.5%, confirming the significance of the model. The statistical significance of the regression models was determined by both the p -value and the F-ratio, which provide a measure of the statistical significance. A high F-ratio value coupled with a low p -value indicates that the equation is statistically significant [15].

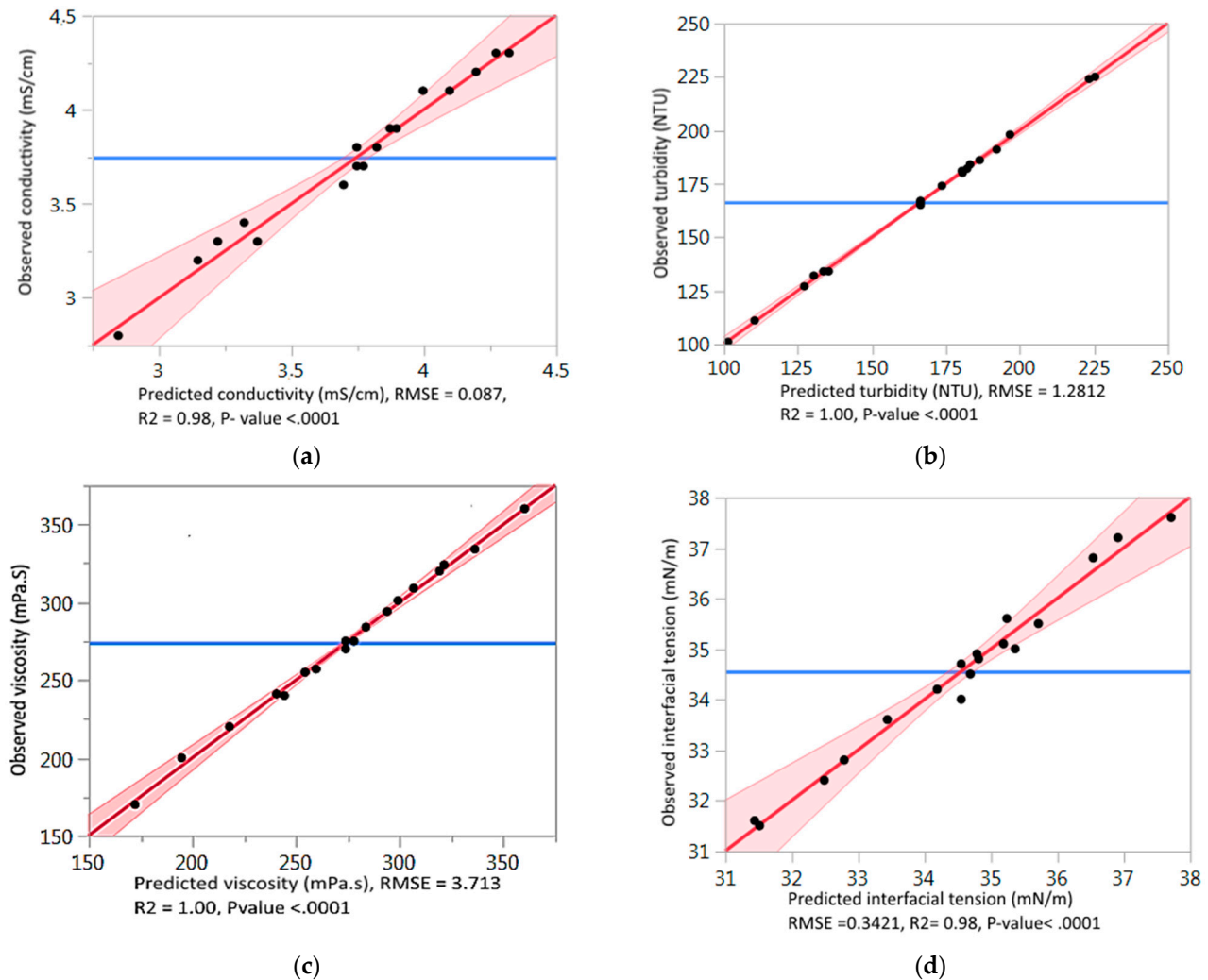


Figure 1. Relation between the observed values and those estimated by the FFD model for (a) conductivity, (b) turbidity, (c) viscosity, and (d) interfacial tension.

The FFD models can evaluate the influence of predictors and their interactions on multiple responses. Table 2 displays the effects of independent variables and their interactions on conductivity, turbidity, viscosity, and interfacial tension. The coefficients for each factor in the model provide insight into their impact on the response [36].

3.1.1. Influence of Independent Variables on the Conductivity

The conventional method to track the interaction between water-soluble polymers and anionic surfactants involves measuring specific or equivalent conductivity and surface tension as a function of surfactant concentration [37].

The assessment of electrostatic interactions in solution, particularly those that involve charged substances such as ionic surfactants, charged polymers, and electrolytes, is a crucial area of research. To investigate these interactions in aqueous mixtures of polymers and surfactants, conductivity measurements were extensively employed. For instance, Goddard et al. [38] employed this method to analyze the impact of salt on the interaction between polyethylene glycol (PEG) and SDS, while Sovilj et al. [39] utilized it to investigate the effects of hydroxypropylmethyl cellulose–SDS interactions.

The iso-response plots from the FFD models shown in Figure 2 display specific conductivity curves at different concentrations of SDBS, kerosene, PEG 1500, and NaCl. These plots depict the effects of two factors while holding the other two factors constant at their zero level.

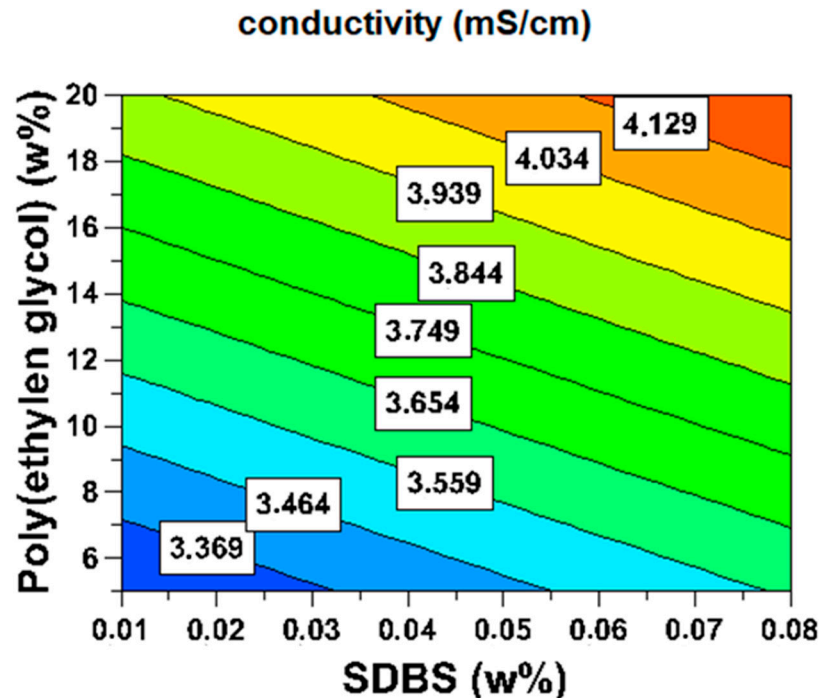


Figure 2. Effect of SDBS and PEG 1500 concentrations on the conductivity (mS/cm): iso-response plot (kerosene 35 w% and NaCl = 1.05 w%).

The method for calculating the specific conductivity of each species at any concentration involves the assumption that the total conductivity of the free ions is unaffected by the presence of any electrolyte in the solution. Therefore, adding together the conductivity of each ion in its presence results in the total specific conductivity of the solution. With this assumption, the specific conductivity of a solution containing the total sodium σ_{Na^+} (the sum of the conductivity of the charged polymer SDBS, PEG, kerosene, and NaCl) can be calculated using Equation (2):

$$\sigma = \sigma_{\text{SDB}^-} + \sigma_{\text{Na}^+} + \sigma_{\text{Kerosene}} + \sigma_{\text{PEG}} + \sigma_{\text{Na}^+} + \sigma_{\text{Cl}^-} \quad (2)$$

The measurement of the total conductivity of the solution, σ , is the only value that can be experimentally obtained from conductivity measurements. Figure 2 illustrates the impact of different factors on conductivity, showing the effects of SDBS and PEG concentrations on conductivity, while keeping the kerosene and NaCl concentrations constant at zero. As expected, the presence of SDBS, an anionic surfactant, slightly increases conductivity as its concentration increases, while the kerosene concentration remains constant at 35 w% and the sodium chloride concentration remains constant at 1.05 w%. With the addition of PEG to the SDBS solutions, the total conductivity of the solution becomes more dependent on the SDBS and NaCl concentrations, as shown in the equation model presented in Table 3. In this case, it is assumed that all ionic species in the solution are completely dissociated, as kerosene and NaCl remain at constant concentrations, and PEG is an uncharged polymer with less influence on conductivity. The highest conductivity value of 4.129 mS/cm is achieved with SDBS at 0.065 w% and PEG at 20 w%.

Figure 3 displays the impact of SDBS and kerosene concentrations on the conductivity, with a constant NaCl concentration of 1.05 w% and PEG concentration of 12.5 w%. In comparison to the previous case, the presence of olive oil, along with SDBS, increases the

conductivity but to a lesser extent. The values range from 3.492 mS/cm for 0.01 w% SDBS and 25 w% kerosene to 4.012 mS/cm for concentrations close to the maximum levels of SDBS and olive oil. When kerosene is added to the SDBS solutions while keeping the PEG and NaCl concentrations constant, the total conductivity of the solution is highly dependent on the charged surfactant SDBS and charged electrolyte NaCl. Similar to the previous case, we assume that all ionic species in the solution are completely dissociated because the NaCl and polymer concentrations are constant.

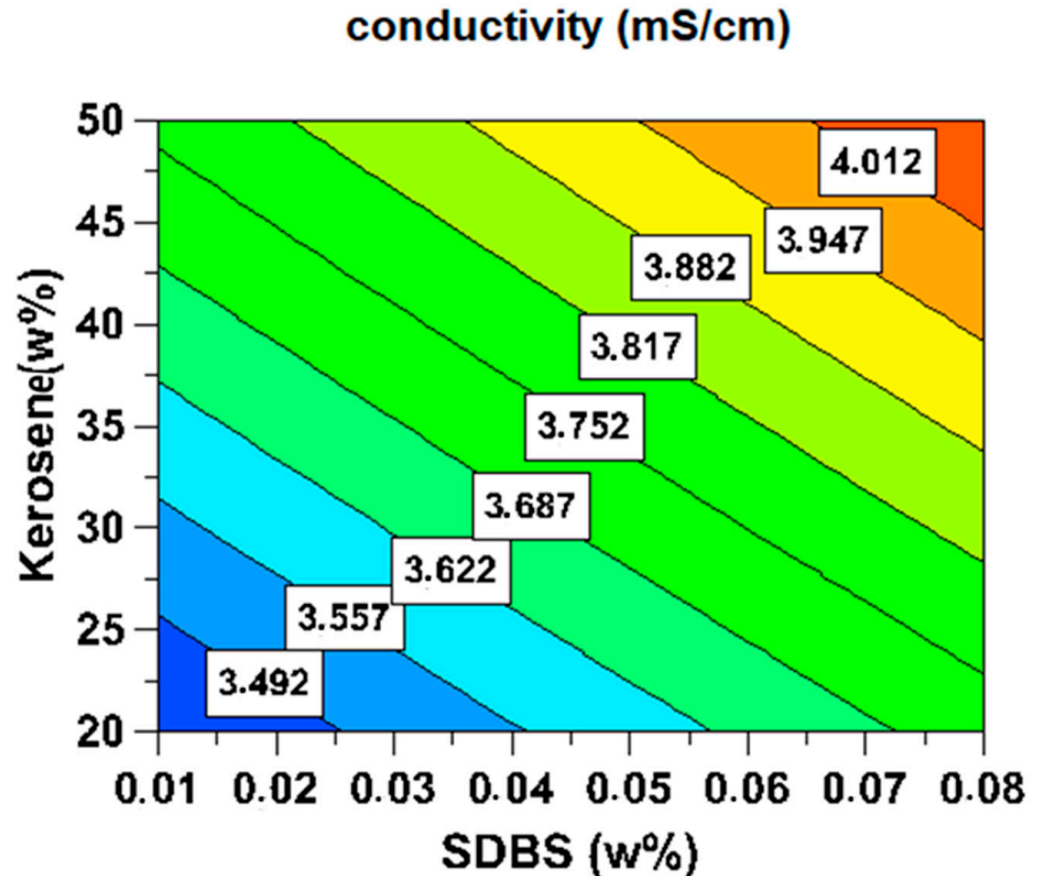


Figure 3. Effect of SDBS and kerosene concentrations on the conductivity; iso-response plot (PEG = 12.5 w% and NaCl = 1.05 w%).

Figure 4 illustrates the effects of SDBS and NaCl concentrations on the conductivity when the concentrations of PEG and kerosene are kept constant at their zero level (PEG = 12.5 w% and kerosene = 35 w%). The presence of NaCl, a charged electrolyte, with SDBS significantly increases the conductivity. The conductivity values range from 3.524 mS/cm for 0.018 w% SDBS and 0.5 w% NaCl concentrations to 3.947 mS/cm for values near the maximum concentrations of SDBS and NaCl. Similar to the previous case, the total conductivity of the solution depends strongly on the charged surfactant SDBS and the charged electrolyte NaCl when kerosene is added to the SDBS solutions at constant PEG and NaCl concentrations. Once again, we assume complete dissociation of all ionic species in the solution due to the constant concentrations of NaCl and polymer.

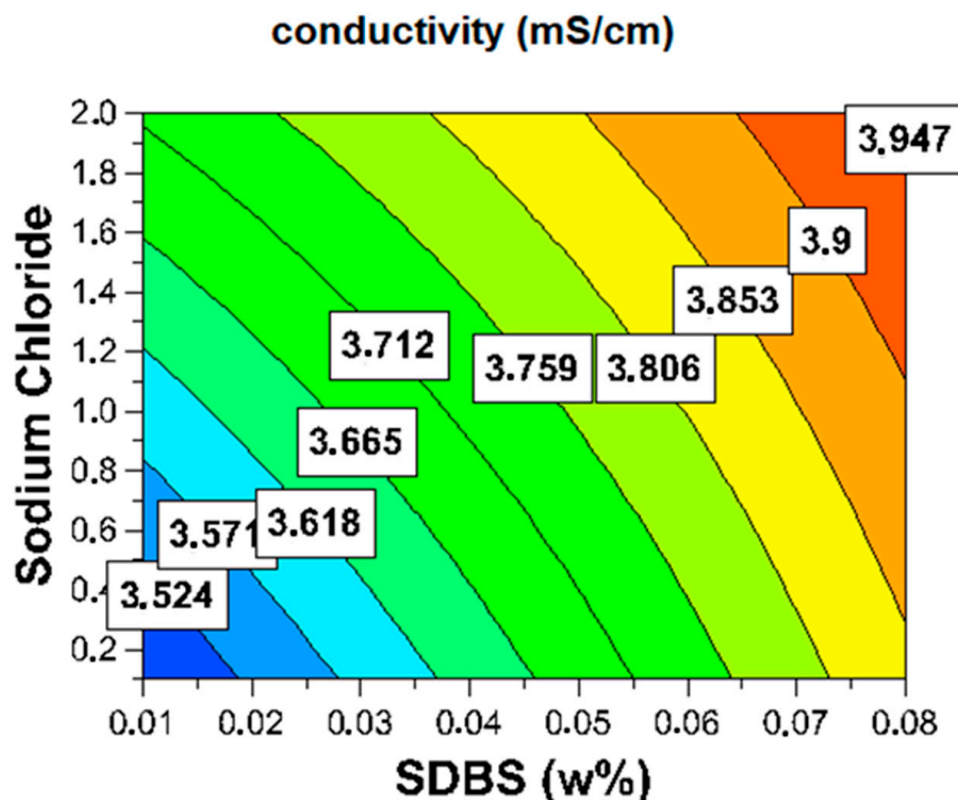


Figure 4. Effect of SDBS and NaCl concentrations on the conductivity; iso-response plot (PEG, 12.5 w%; kerosene, 35 w%).

3.1.2. Influence of Independent Variables on the Turbidity

Turbidity refers to the presence of suspended matter or colloidal particles that disrupt the fluid and can be caused by various factors, such as bacteria, microalgae, or suspended matter in rivers. To determine the transmittance of solutions containing charged polymer, cationic and nonionic surfactants in the presence of oil, a turbidimetric method is used. By using the equation for turbidity in Table 3, turbidity curves can be obtained to represent the effects of varying SDBS and PEG concentrations, while keeping kerosene and NaCl concentrations constant (at 35 w% and 1.05 w%, respectively). The resulting iso-response plots show that the turbidity increases with increasing concentrations of SDBS and PEG, with the maximum turbidity of 181.8 NTU occurring at the highest concentrations of these two substances. The iso-response curves in Figure 5 reveal that PEG concentrations have a significant influence on turbidity, with the minimum turbidity of 149.8 NTU observed at the smallest concentrations.

Figure 6 shows the turbidity level varies with the concentration levels of PEG and kerosene, while SDBS is kept constant at 0.045 w% and NaCl at 1.05 w%. The plot demonstrates the impact of changing concentrations of PEG and kerosene on turbidity levels, while keeping the other two concentrations steady. As expected, the minimum turbidity level of 148 NTU was achieved when the concentrations of PEG and kerosene were at their lowest, and the turbidity increased with the increasing cloudiness of the solution, which is confirmed by the curves in Figure 6. The maximum turbidity level of 196.8 NTU was obtained when PEG and kerosene concentrations were at their maximum levels.

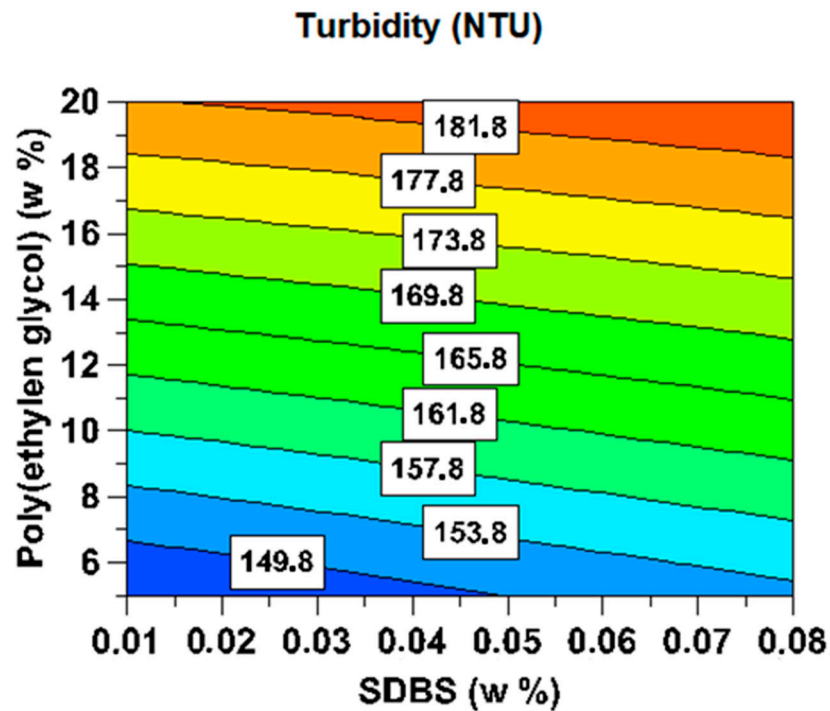


Figure 5. SDBS and PEG concentrations on the turbidity (NTU): iso-response plot (kerosene = 35 w% and NaCl = 1.05 w%).

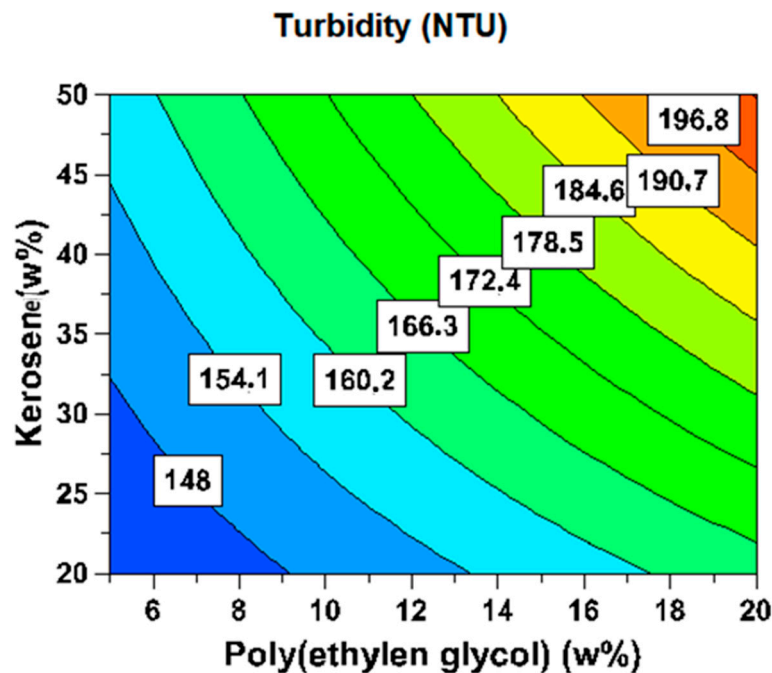


Figure 6. PEG and kerosene concentrations on the turbidity (NTU): iso-response plot SDBS = 0.45 w% and NaCl = 1.05 w%).

3.1.3. Effect of Independent Variables on the Viscosity

The viscosity of the solution is primarily affected by the presence of the PEG polymer and viscosimetric compound kerosene. Therefore, measuring the viscosity is an effective way to study the hydrodynamic volume of the solution. The apparent viscosity (η_{app}) values were determined using the equation presented in Table 3 and plotted in the iso-response plots for viscosity at varying SDBS, PEG, kerosene, and NaCl concentrations. Figure 7 shows that the apparent viscosity values increase as the concentrations of PEG and

kerosene increase. The maximum viscosity value of 320 mPa.s was obtained at the maximum concentration of PEG and a kerosene concentration of about 45 w% at a constant SDBS concentration of 0.45% wt and constant NaCl concentration of 1.05 w%. This behavior can be explained by the dispersion of the charged polymer molecules in the presence of viscous oil, which results in significant changes in viscosity values with increasing concentrations. The interaction between the surfactant micelles and polymer chains can also be attributed to the formation of composite micelles in this region of maximum viscosity [40].

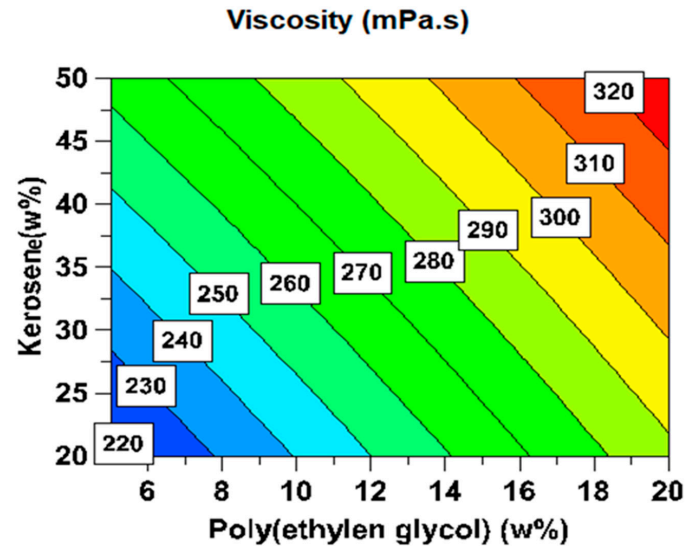


Figure 7. Effect of PEG and kerosene concentrations on the viscosity (mPa/s): iso-response plot (SDBS = 0.45 w% and NaCl = 1.05 w%).

Figure 8 presents the iso-response curves, which demonstrate that viscosity values increase as the concentrations of SDBS and kerosene increase. The maximum viscosity value of 300.9 mPa.s was obtained when the SDBS concentration was around 0.065 w% and the kerosene concentration was about 50 w% at constant concentrations of PEG (12.5 w%) and NaCl (1.05 w%). It is observed that the maximum viscosity value obtained in Figure 8 is lower (300.9 mPa.s) than the maximum value obtained in the previous case (320 mPa.s in Figure 7). This can be explained by the higher viscosity of the polymer and kerosene compared to SDBS, which has a lower viscosity.

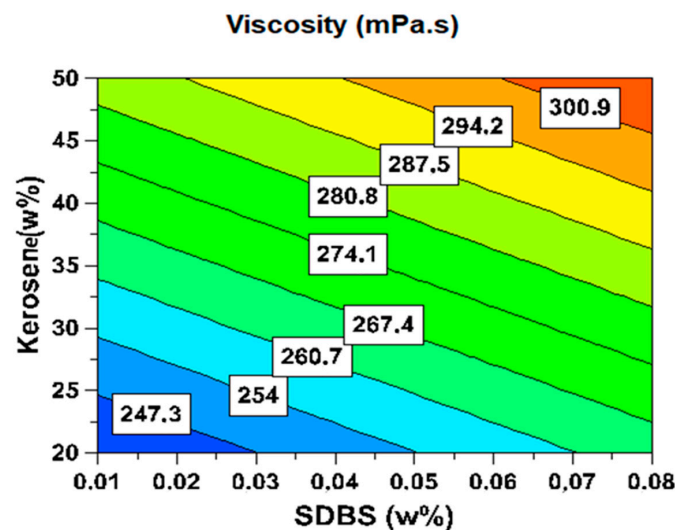


Figure 8. Effect of SDBS and kerosene concentrations on the viscosity (mPa/s): iso-response plot (PEG = 12.5 w% and NaCl = 1.05 w%).

3.1.4. Influence of Independent Variables on the Interfacial Tension

The IFT method is utilized to explain the micellization process of surfactant solutions, the distribution of molecules in the presence of an additive, and the surface activity and micelle formation of ionic surfactants when combined with charged polymers and salt. The influence of independent variables on interfacial tension is used to understand these phenomena. The behavior of surface tension in a multicomponent system can be obtained from classical thermodynamic relationships for interfacial properties, based on the formulation proposed by Gibbs and represented by the following equation [40]:

$$d\gamma = \sum \Gamma_i d\mu_i \quad (3)$$

where γ , Γ_i , and μ_i are the surface or the interfacial tension, surface excess component, and chemical potential of the component ($\mu_i = \mu_i^0 + RT \ln a_i$); μ_i^0 is the standard chemical potential; and a_i is the activity of i .

Using the expression of the chemical potential in Equation (4), the following is obtained for dilute solution ($a_i = C_i$):

$$d\gamma = \sum \Gamma_i d \ln C_i \quad (4)$$

In a mixed multicomponent system of constant composition, we have the following:

$$C_1 = KC_2 = KC_3 \quad (5)$$

Taking logarithm and differentiating, we have the following:

$$d \ln C_1 = d \ln C_2 = d \ln C_3 \quad (6)$$

The Gibbs adsorption equation for a system containing three components (sodium dodecylbenzene sulphonate (SDS), sodium chloride (NaCl), and xanthan gum (XG)) becomes as follows:

$$d\gamma = -RT \left(\Gamma_{CTAB} + \Gamma_{Tween80} + \Gamma_{AlgNa} + \Gamma_{Olive\ Oil} \right) d \ln C_1 \quad (7)$$

For ionic compounds, we assume the complete dissociation of cetyltrimethylammonium bromide CTAB ($CTAB = CTA^+ + Br^-$) and sodium alginate AlgNa ($AlgNa = Alg^- + Na^+$) and the dissociation of Tween 80 and olive oil are negligible; hence, we have the following:

$$\Gamma_{CTAB} + \Gamma_{CTA^+} + \Gamma_{Br^-} \text{ and } \Gamma_{AlgNa} = \Gamma_{Alg^-} + \Gamma_{Na^+} \quad (8)$$

It is assumed that there is positive adsorption, and only the solute occupies the surface, resulting in a surface excess of pure solvent (in this case, water) of $\Gamma_{Solvent} = 0$. Therefore, the change in Γ resulting from a change in concentration of any component can be used to determine the total excess:

$$\Gamma_{tot} = \Gamma_{CTAB} + \Gamma_{AlgNa} + \Gamma_{Tween80} + \Gamma_{Olive\ Oil} \quad (9)$$

In practice, only the overall interfacial tension (IFT), represented by γ , can be determined through interfacial tension measurements. Figure 9 presents the iso-response curves for IFT at varying concentrations of SDBS and PEG, while the concentrations of kerosene and NaCl are held at their zero level. As expected, the IFT values decrease with increasing SDBS concentrations and increase with increasing PEG concentrations. The minimum IFT iso-response curve, equal to 33.75 mN/m, is achieved at an SDBS concentration of 0.045 w% and PEG concentration of 19 w%. The addition of poly(ethylene glycol) reduces the critical micellar concentration (cmc) of SDBS and increases the aggregation number of individual micelles at higher polymer concentrations. Furthermore, the addition of polymer to SDBS solution lowers the concentration of critical aggregation (CAC) and increases the size and number of the micellar aggregates that attach to the polymer coil. This suggests that a stronger effect of surfactant presence is expected in solutions with polymer. Conversely, excess sodium ions in the solution should screen the electrostatic repulsions between micellar

aggregates attached to the polymer chain, reducing the degree of expansion. Despite the electrolytic affinity of the dissolved PEG molecule, the presence of Na^+ does not affect the extension thickening behavior of the solutions [39,41,42].

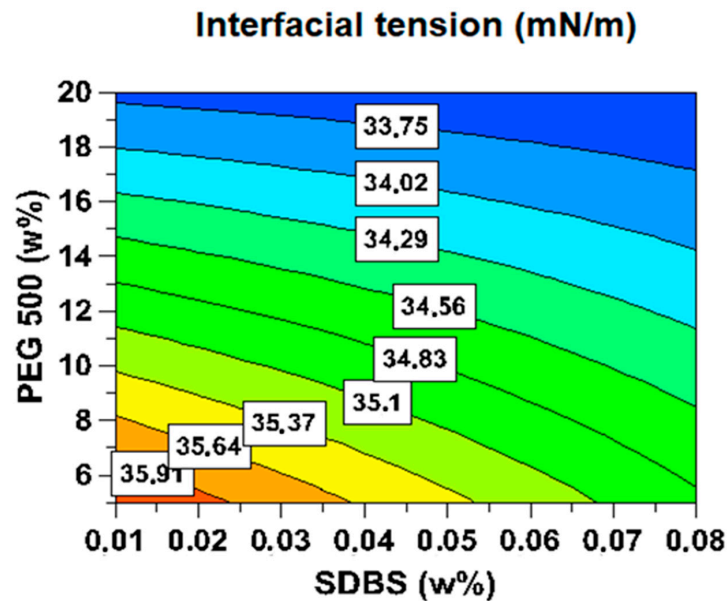


Figure 9. Effect of SDBS and PEG concentrations on the IFT (mN/m): iso-response plot (kerosene = 35 w% and NaCl = 1.05 w%).

Figure 10 shows the relationship between the concentrations of SDBS and kerosene and surface tension while keeping the concentrations of PEG and NaCl constant. It is observed that as the concentration of SDBS and kerosene increases, the surface tension decreases. The lowest value of surface tension, 34.226 mN/m, is attained at a SDBS concentration of 0.075 w% and a kerosene concentration close to 50 w%. This trend is similar to the one observed in Figure 9, where the effect of SDBS and PEG concentrations on interfacial tension is shown. The decrease in surface tension with the increasing SDBS concentration is typical behavior of amphiphilic compounds, which tend to reduce the surface tension at the interface. The iso-response plots in Figures 9 and 10 confirm this hypothesis.

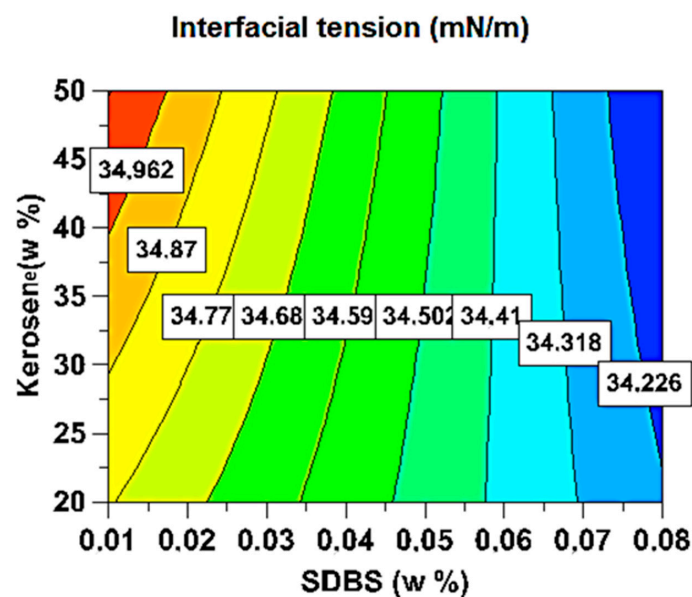


Figure 10. Effect of SDBS and kerosene concentrations on the IFT (mN/m): iso-response plot (PEG = 12.5 w%, NaCl = 1.05 w%).

3.2. Multi-Objective Optimization

The primary aim of this study was to identify the optimal concentrations of SDBS, kerosene, PEG, and sodium chloride that result in the best system performance. To achieve this, the study used multi-objective optimization (MOO) to solve the optimization problem. The four objectives were assigned weights, and their weighted sum was considered as a single objective, which was solved using the particle swarm algorithm available in the MATLAB Optimization Toolbox [16]. The objective functions considered in this study were the minimum conductivity (J_1), the minimum turbidity (J_2), the minimum viscosity (J_3), and the minimum interfacial tension (J_4). These objectives were combined into a scalar goal as follows:

$$J = w_1J_1 + w_2J_2 + w_3J_3 + w_4J_4 \quad (10)$$

where w_1 , w_2 , w_3 , and w_4 are weighting factors, which can be calculated using the rank sum method [16,43–45].

The study assigns weights to the four objective functions, namely J_1 , J_2 , J_3 , and J_4 , which are all given an equal weight of 0.25. The kerosene concentration is constrained between its minimum value (20%) and maximum value (50%). Once the optimal conditions are determined, an experimental validation is carried out to assess the validity of the optimal conditions. The results of this validation are presented in Table 4 to compare them to the predicted values and to express the error between them. In Table 4, the error is defined as follows:

$$Error = Experimental\ response - Predicted\ response \quad (11)$$

Table 4. Comparison between actual and predicted response at optimum condition.

	J_1	J_2	J_3	J_4	J
SDBS (%w) = 0.01, kerosene (%w) = 20, PEG (%w) = 5, and NaCl (%w) = 0.1					
Experimental	2.8	101	170	37.6	77.8500
Predicted response	2.8473	102.1710	174.1447	44.7650	80.98
Error	0.0473	1.1710	4.1447	7.1650	3.1300
SDBS (%w) = 0.01, kerosene (%w) = 50, PEG (%w) = 5, and NaCl (%w) = 0.1					
Experimental	3.4	127	220	37.2	96.9000
Predicted response	3.3973	126.6710	217.3947	43.9026	97.8414
Error	0.0027	0.3290	2.6053	6.7026	0.9414

Table 4 shows that the optimal conditions for both concentrations of kerosene are identical with a negligible margin of error between the predicted and experimental values. This discovery demonstrates that the output models are highly effective and in strong accordance with the experimental outcomes.

4. Conclusions

The present work investigated the effect of surfactants, polymers, oils, and electrolytes on the physicochemical properties of the studying system. A full factorial design was used to optimize the process parameters, and the results showed that the optimal conditions for all four outputs were SDBS (%w) = 0.01, kerosene (%w) = 50, PEG (%w) = 5, and NaCl (%w) = 0.1. The developed models were validated through experimental results and demonstrated high efficiency and accuracy while predicting the response variables. The study provides an important insight into the behavior of surfactants, polymers, oils,

and electrolytes in the system and can have potential applications in various industries, such as mineral extraction, wastewater treatment, and oil recovery. The developed models can be used to improve the efficiency and reduce the cost of these processes through a multi-objective optimization framework. Future research can focus on investigating the effect of other parameters, such as temperature and pH, on the physicochemical properties of the system. In addition, the developed models can be further validated in different experimental conditions and with different surfactants, polymers, oils, and electrolytes to increase their robustness and extend their applicability to other fields.

Author Contributions: Conceptualization: M.N., N.N., M.K., H.T., R.B., A.A.A., A.A., B.J., J.Z. and L.M.; Methodology: M.N., N.N., M.K., R.B., A.A.A., A.A., B.J., J.Z. and L.M.; Software: H.T. and J.Z.; Validation: M.K., H.T., R.B., A.A.A., A.A., B.J. and J.Z.; Data curation: M.N., H.T., A.A. and J.Z.; Formal analysis: M.K., H.T., A.A.A., A.A., J.Z. and L.M.; Resources: M.N., N.N., M.K., R.B., A.A., B.J. and L.M.; Writing—original draft: M.N., N.N., M.K., H.T. and M.K.; Writing—review & editing: H.T., R.B., A.A.A., A.A., B.J., J.Z. and L.M. Investigation: M.N., N.N., M.K., R.B., A.A.A., A.A., B.J., J.Z. and L.M.; Visualization: M.N., N.N., M.K., H.T., R.B., A.A.A., A.A., B.J., J.Z. and L.M.; Supervision: N.N., A.A. and J.Z.; Project administration: M.N., N.N., A.A. and J.Z. All authors have read and agreed to the published version of the manuscript.

Funding: This research received no external funding.

Institutional Review Board Statement: Not applicable.

Informed Consent Statement: Not applicable.

Data Availability Statement: The data presented in this study are available in the manuscript.

Conflicts of Interest: The authors declare no conflict of interest.

References

1. García-Mateos, I.; Pérez, S.; Velázquez, M.M. Interaction between Cetyl Pyridinium Chloride and Water-Soluble Polymers in Aqueous Solutions. *J. Colloid Interface Sci.* **1997**, *194*, 356–363. [[CrossRef](#)] [[PubMed](#)]
2. Avranas, A.; Iliou, P. Interaction between Hydroxypropylmethylcellulose and the Anionic Surfactants Hexane-, Octane-, and Decanesulfonic Acid Sodium Salts, as Studied by Dynamic Surface Tension Measurements. *J. Colloid Interface Sci.* **2003**, *258*, 102–109. [[CrossRef](#)]
3. Smitter, L.M.; Guedez, J.F.; Müller, A.J.; Saez, A.E. Interactions between Poly (Ethylene Oxide) and Sodium Dodecyl Sulfate in Elongational Flows. *J. Colloid Interface Sci.* **2001**, *236*, 343–353. [[CrossRef](#)]
4. Gilanyi, T.; Wolfram, E. Interaction of Ionic Surfactants with Polymers in Aqueous Solution. *Colloids Surf.* **1981**, *3*, 181–198. [[CrossRef](#)]
5. Barreiro-Iglesias, R.; Alvarez-Lorenzo, C.; Concheiro, A. Poly (Acrylic Acid) Microgels (Carbopol® 934)/Surfactant Interactions in Aqueous Media: Part I: Nonionic Surfactants. *Int. J. Pharm.* **2003**, *258*, 165–177. [[CrossRef](#)] [[PubMed](#)]
6. Cosgrove, T.; Mears, S.J.; Obey, T.; Thompson, L.; Wesley, R.D. Polymer, Particle, Surfactant Interactions. *Colloids Surf. Physicochem. Eng. Asp.* **1999**, *149*, 329–338. [[CrossRef](#)]
7. Minatti, E.; Zanette, D. Salt Effects on the Interaction of Poly (Ethylene Oxide) and Sodium Dodecyl Sulfate Measured by Conductivity. *Colloids Surf. Physicochem. Eng. Asp.* **1996**, *113*, 237–246. [[CrossRef](#)]
8. Guo, W.; Sun, Y.W.; Luo, G.S.; Wang, Y.J. Interaction of PEG with Ionic Surfactant SDS to Form Template for Mesoporous Material. *Colloids Surf. Physicochem. Eng. Asp.* **2005**, *252*, 71–77. [[CrossRef](#)]
9. Feng, Q.; Wang, M.; Zhang, G.; Zhao, W.; Han, G. Enhanced Adsorption of Sulfide and Xanthate on Smithsonite Surfaces by Lead Activation and Implications for Flotation Intensification. *Sep. Purif. Technol.* **2023**, *307*, 122772. [[CrossRef](#)]
10. Feng, Q.; Yang, W.; Wen, S.; Wang, H.; Zhao, W.; Han, G. Flotation of Copper Oxide Minerals: A Review. *Int. J. Min. Sci. Technol.* **2022**. [[CrossRef](#)]
11. Puvvada, S.; Blankschtein, D. Molecular-thermodynamic Approach to Predict Micellization, Phase Behavior and Phase Separation of Micellar Solutions. I. Application to Nonionic Surfactants. *J. Chem. Phys.* **1990**, *92*, 3710–3724. [[CrossRef](#)]
12. Nedjhioui, M.; Moulai-Mostefa, N.; Sellami, A.; Toubal, F. Contribution to the Study of the Combined Effects of Aqueous Solution Containing Surfactants and Biopolymers on Some Physical and Rheological Parameters. *Desalination Water Treat.* **2015**, *56*, 2739–2745. [[CrossRef](#)]
13. Montgomery, D.C. *Montgomery: Design and Analysis of Experiments*; John Wiley Sons: Hoboken, NJ, USA, 2017.
14. Tahraoui, H.; Belhadj, A.E.; Moula, N.; Bouranene, S.; Amrane, A. Optimisation and Prediction of the Coagulant Dose for the Elimination of Organic Micropollutants Based on Turbidity. *Kem. U Ind.* **2021**. [[CrossRef](#)]

15. Bouchelkia, N.; Tahraoui, H.; Amrane, A.; Belkacemi, H.; Bollinger, J.-C.; Bouzaza, A.; Zoukel, A.; Zhang, J.; Mouni, L. Jujube Stones Based Highly Efficient Activated Carbon for Methylene Blue Adsorption: Kinetics and Isotherms Modeling, Thermodynamics and Mechanism Study, Optimization via Response Surface Methodology and Machine Learning Approaches. *Process Saf. Environ. Prot.* **2022**. [[CrossRef](#)]
16. Tahraoui, H.; Belhadj, A.-E.; Triki, Z.; Boudella, N.R.; Seder, S.; Amrane, A.; Zhang, J.; Moula, N.; Tifoura, A.; Ferhat, R.; et al. Mixed Coagulant-Flocculant Optimization for Pharmaceutical Effluent Pretreatment Using Response Surface Methodology and Gaussian Process Regression. *Process Saf. Environ. Prot.* **2022**, S0957582022010102. [[CrossRef](#)]
17. Kothari, C.R. *Research Methodology: Methods and Techniques*; New Age International: Shahjahanabad, India, 2004; ISBN 81-224-1522-9.
18. Bouyahia, C.; Rahmani, M.; Benslemli, M.; El Hajjaji, S.; Slaoui, M.; Bencheikh, I.; Azoulay, K.; Labjar, N. Influence of Extraction Techniques on the Adsorption Capacity of Methylene Blue on Sawdust: Optimization by Full Factorial Design. *Mater. Sci. Energy Technol.* **2023**, *6*, 114–123. [[CrossRef](#)]
19. Oimoen, S. *Classical Designs: Full Factorial Designs*; STAT Center of Excellence: Dayton, OH, USA, 2019.
20. Braima, N.; Maryam, A.N.A.; Odejebi, O.J. Utilization of Response Surface Methodology (RSM) in the Optimization of Crude Oil Refinery Process, New Port-Harcourt Refinery, Nigeria. *J. Multidiscip. Eng. Sci. Technol.* **2016**.
21. Nedjhioui, M.; Moulai-Mostefa, N.; Canselier, J.P.; Bensmaili, A. Investigation of Combined Effects of Xanthan Gum, Sodium Dodecyl Sulphate, and Salt on Some Physicochemical Properties of Their Mixtures Using a Response Surface Method. *J. Dispers. Sci. Technol.* **2009**, *30*, 1333–1341. [[CrossRef](#)]
22. Maaze, M.R.; Shrivastava, S. Design Development of Sustainable Brick-Waste Geopolymer Brick Using Full Factorial Design Methodology. *Constr. Build. Mater.* **2023**, *370*, 130655. [[CrossRef](#)]
23. Nedjhioui, M.; Moulai-Mostefa, N.; Morsli, A.; Bensmaili, A. Combined Effects of Polymer/Surfactant/Oil/Alkali on Physical Chemical Properties. *Desalination* **2005**, *185*, 543–550. [[CrossRef](#)]
24. Nedjhioui, M.; Canselier, J.-P.; Moulai-Mostefa, N.; Bensmaili, A.; Skender, A. Determination of Micellar System Behavior in the Presence of Salt and Water-Soluble Polymers Using the Phase Diagram Technique. *Desalination* **2007**, *206*, 589–593. [[CrossRef](#)]
25. Moulai-Mostefa, N.; Khalladi, R.; Nedjhioui, M. An Investigation into the Interactions between a Polymer and a Surfactant Using Viscosity, Conductivity and Surface Tension Measurements. *Proc. Ann. De Chim. Paris 1914* **2007**, *32*, 421–429. [[CrossRef](#)]
26. Nedjhioui, M.; Moulai-Mostefa, N.; Tir, M. Effect of Some Physical and Chemical Properties on the Interactions between Biopolymers and Anionic Surfactants. *Desalination Water Treat.* **2015**, *55*, 3704–3712. [[CrossRef](#)]
27. Yahoum, M.M.; Toumi, S.; Hentabli, S.; Tahraoui, H.; Lefnaoui, S.; Hadjsadok, A.; Amrane, A.; Kebir, M.; Moula, N.; Assadi, A.A. Experimental Analysis and Neural Network Modeling of the Rheological Behavior of Xanthan Gum and Its Derivatives. *Materials* **2023**, *16*, 2565. [[CrossRef](#)] [[PubMed](#)]
28. Hadadi, A.; Imessaoudene, A.; Bollinger, J.-C.; Bouzaza, A.; Amrane, A.; Tahraoui, H.; Mouni, L. Aleppo Pine Seeds (*Pinus Halepensis* Mill.) as a Promising Novel Green Coagulant for the Removal of Congo Red Dye: Optimization via Machine Learning Algorithm. *J. Environ. Manag.* **2023**, *331*, 117286. [[CrossRef](#)]
29. Tahraoui, H.; Belhadj, A.-E.; Hamitouche, A.; Bouhedda, M.; Amrane, A. Predicting the Concentration of Sulfate (So₄²⁻) in Drinking Water Using Artificial Neural Networks: A Case Study: Médéa-Algeria. *Desalination Water Treat.* **2021**, *217*, 181–194. [[CrossRef](#)]
30. Zamouche, M.; Tahraoui, H.; Laggoun, Z.; Mechat, S.; Chemchmi, R.; Kanjal, M.I.; Amrane, A.; Hadadi, A.; Mouni, L. Optimization and Prediction of Stability of Emulsified Liquid Membrane (ELM): Artificial Neural Network. *Processes* **2023**, *11*, 364. [[CrossRef](#)]
31. Bousselma, A.; Abdessemed, D.; Tahraoui, H.; Amrane, A. Artificial Intelligence and Mathematical Modelling of the Drying Kinetics of Pre-Treated Whole Apricots. *Kem. U Ind.* **2021**. [[CrossRef](#)]
32. Tahraoui, H.; Belhadj, A.E.; Hamitouche, A.E. Prediction of the Bicarbonate Amount in Drinking Water in the Region of Médéa Using Artificial Neural Network Modelling. *Kem. U Ind.* **2020**, *69*, 595–602. [[CrossRef](#)]
33. Tahraoui, H.; Amrane, A.; Belhadj, A.-E.; Zhang, J. Modeling the Organic Matter of Water Using the Decision Tree Coupled with Bootstrap Aggregated and Least-Squares Boosting. *Environ. Technol. Innov.* **2022**, *27*, 102419. [[CrossRef](#)]
34. Tahraoui, H.; Belhadj, A.-E.; Amrane, A.; Houssein, E.H. Predicting the Concentration of Sulfate Using Machine Learning Methods. *Earth Sci. Inform.* **2022**, *15*, 1023–1044. [[CrossRef](#)]
35. Zamouche, M.; Chermat, M.; Kermiche, Z.; Tahraoui, H.; Kebir, M.; Bollinger, J.-C.; Amrane, A.; Mouni, L. Predictive Model Based on K-Nearest Neighbor Coupled with the Gray Wolf Optimizer Algorithm (KNN_GWO) for Estimating the Amount of Phenol Adsorption on Powdered Activated Carbon. *Water* **2023**, *15*, 493. [[CrossRef](#)]
36. Singh, B.; Kumar, P. Pre-Treatment of Petroleum Refinery Wastewater by Coagulation and Flocculation Using Mixed Coagulant: Optimization of Process Parameters Using Response Surface Methodology (RSM). *J. Water Process Eng.* **2020**, *36*, 101317. [[CrossRef](#)]
37. Lefnaoui, S.; Moulai-Mostefa, N. Investigation and Optimization of Formulation Factors of a Hydrogel Network Based on Kappa Carrageenan–Pregelatinized Starch Blend Using an Experimental Design. *Colloids Surf. Physicochem. Eng. Asp.* **2014**, *458*, 117–125. [[CrossRef](#)]
38. Langevin, D. Polyelectrolyte and Surfactant Mixed Solutions. Behavior at Surfaces and in Thin Films. *Adv. Colloid Interface Sci.* **2001**, *89*, 467–484. [[CrossRef](#)] [[PubMed](#)]
39. Goddard, E.D. Polymer—Surfactant Interaction Part I. Uncharged Water-Soluble Polymers and Charged Surfactants. *Colloids Surf.* **1986**, *19*, 255–300. [[CrossRef](#)]

40. Harrison, I.M.; Candau, F.; Zana, R. Interactions between Polyampholytes and Ionic Surfactants. *Colloid Polym. Sci.* **1999**, *277*, 48–57. [[CrossRef](#)]
41. Ghosh, S.; Moulik, S.P. Interfacial and Micellization Behaviors of Binary and Ternary Mixtures of Amphiphiles (Tween-20, Brij-35, and Sodium Dodecyl Sulfate) in Aqueous Medium. *J. Colloid Interface Sci.* **1998**, *208*, 357–366. [[CrossRef](#)]
42. Sovilj, V.J.; Petrović, L.B. Influence of Hydroxypropylmethyl Cellulose–Sodium Dodecylsulfate Interaction on the Solution Conductivity and Viscosity and Emulsion Stability. *Carbohydr. Polym.* **2006**, *64*, 41–49. [[CrossRef](#)]
43. Einhorn, H.J.; McCoach, W. A Simple Multiattribute Utility Procedure for Evaluation. *Behav. Sci.* **1977**, *22*, 270–282. [[CrossRef](#)]
44. Dobrosz-Gómez, I.; Gómez García, M.Á.; Gaviria, G.H.; GilPavas, E. Mineralization of Cyanide Originating from Gold Leaching Effluent Using Electro-Oxidation: Multi-Objective Optimization and Kinetic Study. *J. Appl. Electrochem.* **2020**, *50*, 217–230. [[CrossRef](#)]
45. Merta, J.; Stenius, P.; Pirttinen, E. Interactions between Cationic Starch and Anionic Surfactants III Rheology and Structure of the Complex Phase. *J. Dispers. Sci. Technol.* **1999**, *20*, 677–697. [[CrossRef](#)]

Disclaimer/Publisher’s Note: The statements, opinions and data contained in all publications are solely those of the individual author(s) and contributor(s) and not of MDPI and/or the editor(s). MDPI and/or the editor(s) disclaim responsibility for any injury to people or property resulting from any ideas, methods, instructions or products referred to in the content.